

*promoting access to White Rose research papers*



**Universities of Leeds, Sheffield and York**  
**<http://eprints.whiterose.ac.uk/>**

---

This is an author produced version of a paper published in **Journal of Hydrology**

White Rose Research Online URL for this paper:

<http://eprints.whiterose.ac.uk/id/eprint/77450>

---

**Paper:**

Ballard, CE, McIntyre, N, Wheater, HS, Holden, J and Wallage, ZE (2011)  
*Hydrological modelling of drained blanket peatland*. *Journal of Hydrology*, 407 (1-4). 81 - 93. ISSN 0022-1694

<http://dx.doi.org/10.1016/j.jhydrol.2011.07.005>

---

# 1 **Hydrological modelling of drained blanket peatland**

2 <sup>1</sup>Ballard, C., <sup>1</sup>McIntyre, N., <sup>1</sup>Wheater, H., <sup>2</sup>Holden, J. and <sup>3</sup>Wallage, Z.E.

3 <sup>1</sup>Department of Civil and Environmental Engineering, Imperial College London, SW7 2AZ, UK

4 <sup>2</sup>School of Geography, University of Leeds, Leeds, LS2 9JT, UK

5 <sup>3</sup>Low Carbon Innovation Centre, University of East Anglia, Norwich, NR4 2TJ

## 6 **Abstract**

7 Open ditch drainage is a commonly implemented land management practice in upland blanket peatlands,  
8 particularly in the UK, where policy decisions between the 1940s and 1970s lead to widespread drainage  
9 of the uplands. The change in the hydrological regime associated with the drainage of blanket peat is  
10 poorly understood, yet has perceived importance for flooding, low flows and water quality. We propose a  
11 new simplified physics-based model that allows the exploration of the associated hydrological processes  
12 and flow responses. The model couples four one-dimensional models to represent a three-dimensional  
13 hillslope, allowing for the exploration of flow and water table response throughout the model domain for  
14 a range of drainage configurations and peat properties. The model is tested against a data set collected  
15 from Oughtershaw Beck, UK, with results showing good model performance for wet periods although  
16 less compatibility with borehole observations during rewetting periods. A wider exploration of the model  
17 behaviour indicates that the model is consistent with the drained blanket peat hydrological response  
18 reported in the literature for a number of sites, and therefore has potential to provide guidance to decision  
19 makers concerning the effects of management practices. Through a global sensitivity analysis, we  
20 conclude that further field investigations to assist in the surface and drain roughness parameterisation  
21 would help reduce the uncertainty in the model predictions.

22

23 **Keywords:** peatlands, runoff, water table, ditches, drainage, modelling

## 24 **1. Introduction**

25 Peatlands are located across the globe, from the tropics to the high latitudes, covering approximately 3%  
26 of the Earth's surface. These environments are of particular nature conservation value due to their unique  
27 and diverse biodiversity. Moreover, they store soil carbon and water; it is estimated that 10% of the  
28 world's freshwater resources and up to one-third of global soil carbon are stored in peatlands (Rubec,  
29 2005).

30  
31 In the UK, 87 % of peat covered areas take the form of blanket peat. The UK uplands include  
32 approximately 2.9 M ha of blanket peatland (Holden et al., 2004), constituting approximately 15% of the  
33 global amount of blanket peatland (Milne and Brown, 1997). These regions have traditionally been  
34 heavily managed for low density farming, energy, forestry and game rearing. In recent times, in  
35 recognition of the significant ecosystem services provided by peatlands (including biodiversity, carbon  
36 sequestration, water supply, and recreation (Bonn et al., 2009)), many areas of upland blanket peatland  
37 have been designated as 'Sites of Special Scientific Interest', 'Areas of Outstanding Natural Beauty',  
38 'Special Protection Areas', 'Environmentally Sensitive Areas', 'Special Areas of Conservation' and  
39 National Nature Reserves (Condliffe, 2009). Peatlands also generate a large proportion of the UK water  
40 supply; therefore water quality and colour are also significant considerations (Armstrong et al., 2010).  
41 The management of these areas is thus of interest to a range of stakeholders, including physical and  
42 social scientists, and land owners and managers. Given the inherent significance of the upper areas of  
43 catchments for downstream flooding, with their higher rainfall rates and generally flashier response  
44 (Wheater et al., 2008), the management of upland blanket peatland also has the potential to affect flood  
45 risk.

46  
47 In the UK, approximately 50% of upland blanket peatland has been drained (Milne and Brown, 1997),  
48 which in England alone amounts to 75,000 ha. Drainage of peats is typically via a series of open ditches,  
49 with the aim of improving vegetation and therefore the production of livestock and game (Stewart and  
50 Lance, 1983). The rationale is that drainage will remove excess surface runoff and lower the water table,

51 thereby creating more conducive environments for plant species suitable for stock grazing. However,  
52 these predicted benefits have rarely been realised since blanket peat cannot sustain anything above very  
53 small sheep populations without undergoing severe degradation (Stewart and Lance, 1983); and peatland  
54 drainage is also generally considered to have adverse effects on the natural environment.

55  
56 The implementation of an open ditch drainage scheme causes two key processes to occur: (1) water is  
57 drained from the soil matrix directly into the open drains, lowering water tables and creating more soil  
58 storage capacity, and (2) surface runoff and direct rainfall are captured in the drains and transmitted to  
59 the catchment outlet more rapidly (Holden, 2009b). How peatland drainage affects flooding in the  
60 catchment depends on the interaction of these two counteracting processes, where process (1) tends to  
61 reduce storm peaks and increase base flows, while process (2) tends to increase the flashiness of the  
62 response and increase peak flows. The dominance of each process is likely to depend on a number of  
63 factors including: drainage density and geometry, hydraulic conductivity, drain and peat surface  
64 roughnesses, topography, event size, and antecedent conditions.

65  
66 Observations have shown that drained peatlands typically have a shorter time to peak, higher peak flow  
67 and a quicker recession than undrained areas, and are associated with increased water table fluctuations  
68 (Ahti, 1980; Conway and Millar, 1960; Holden et al., 2006; Robinson, 1986; Stewart and Lance, 1991).  
69 The zone of influence of the water table drawdown (i.e. process (1) above) due to the drains is quite  
70 limited in blanket peats, due to very low hydraulic conductivities, particularly in the deeper layers  
71 (Robinson, 1986; Stewart and Lance, 1983), therefore the spacing of the drains plays a significant role in  
72 both the short and long term effects of drainage. The effect is also not uniform in space, particularly in  
73 blanket peat on sloping terrains, since the reduction in upslope contributing area is most significant  
74 immediately downslope of a drain (Coulson et al., 1990; Holden et al., 2006). In a minority of field  
75 studies, drainage of peatlands has been observed to decrease flood peaks (e.g. Burke, 1967; Coulson et  
76 al., 1990; Newson and Robinson, 1983). However, in all of these cases some aspects of the site  
77 conditions are at the extreme of the range of conditions that are typically encountered in drained  
78 peatlands. For example, Burke (1967) studied a site with especially dense (3.5m) drain spacing and

79 drains running along contours, thus minimising drain flow velocity; Newson and Robinson (1983)  
80 examined a peaty soil with a hydraulic conductivity higher than typical blanket peats; and Coulson  
81 (1990) studied a site with lower altitude and lower annual rainfall than typical for UK peatlands.  
82  
83 Given the uncertainty about best management practices for peatlands, due largely to the complexity of  
84 process interactions, there is a need for suitable process-based models to aid understanding of impacts of  
85 management interventions. Due to the difficulties in observing and quantifying land management effects  
86 at the catchment scale, the simplest case to consider is the response at field or hillslope scales. Some  
87 modelling has been performed to examine drainage in the uplands, notably hillslope simulations using  
88 SHETRAN (Dunn and Mackay, 1996) and a modified TOPMODEL (Lane, 2002; Lane et al., 2004; Lane  
89 et al., 2003). However, while the TOPMODEL simulations can explicitly represent drainage networks,  
90 the conceptual nature of the model does not provide detail about the subsurface behaviour, particularly at  
91 the sub-drain spacing scale. The conceptual stores in the model that represent saturated subsurface  
92 storage are independent of each other, hence, although the topographic index concept partly  
93 accommodates the way a cell may be affected by upslope areas, downslope effects, such as the presence  
94 of drains and the level of water in them, cannot be simulated. The studies have also not been compared  
95 against any observed flow or water table time series. The SHETRAN simulations of Dunn and Mackay  
96 (1996) are physically based, but the drainage configurations were limited to alignments with the grid  
97 boundaries (due to their representation as ‘channel elements’), thereby providing a limited range of  
98 potential drain configurations. Also, the inter-drain regions were represented by a single grid cell, not  
99 allowing examination of the local changes in water table heights. Hence, although both approaches had  
100 some success at the large scale, in order to explore and examine the hydrological processes associated  
101 with the management of drained peatlands there is a need for a physics-based model that provides  
102 flexibility in the representation of drainage configurations and can provide information about the spatial  
103 variability of the internal model states.  
104  
105 In this paper, a new fine resolution simplified physics-based model is proposed to test hypotheses about  
106 hydrological processes and to investigate the effects of peatland land management. The new model aims

107 to allow the impacts of management scenarios to be explored, as an extension to the limited experimental  
108 data currently available, and as a complement to any future extensive experimental programmes. The  
109 model is tested against flow and water table data from a drained peatland site in the UK. The results from  
110 the analysis are used to explore the model performance and to identify processes that require refinement  
111 and the data that would reduce the uncertainties in the model predictions. Finally, the wider applicability  
112 of the model is assessed.

## 113 **2. Model description**

114 The modelling approach used in this study was to identify the key hydrological processes for intact and  
115 drained peatlands from the literature and include them in a model that has an appropriate level of  
116 complexity relative to the level of information available on the system hydrological processes. To avoid  
117 over-parameterisation, minor processes have been excluded or treated in a simplified manner. In  
118 particular, the development has focused primarily on ombrotrophic (rain water fed) blanket peatlands in  
119 the UK, where deep groundwater flows are expected to be negligible, and on representing processes  
120 known to influence flood generation.

### 121 **2.1. Conceptual model**

122 Blanket peat deposits are typically found draped over gently rolling terrain in areas with a cool climate,  
123 high rainfall and impeded substrate drainage. These conditions allow peat formation, which occurs when  
124 organic material decomposes slowly due to anaerobic conditions associated with waterlogging (Allaby,  
125 2008). Typically, peats exhibit two major zones: the upper layer (acrotelm), which is composed of live  
126 and decaying plant material and can range from 5 to 50 cm thick, and a lower zone (catotelm), which is  
127 denser, usually saturated and anoxic (Evans et al., 1999; Holden and Burt, 2003b; Ingram 1978, 1983).

128

129 Water tables in blanket peat catchments are generally observed to fluctuate between the top of the  
130 catotelm and the ground surface and are highly responsive to changes in the soil water balance (Evans et  
131 al., 1999). Due to these typically high water tables, soil water storage does not contribute significantly to  
132 the attenuation of winter floods and surface runoff in peat catchments is generally observed to be due to

133 saturation excess (Holden and Burt, 2002a). These local scale responses lead to very flashy responses at  
134 the catchment scale (Bragg, 2002; Evans et al., 1999; Holden and Burt, 2003c; Holden et al., 2001) and  
135 generally low base flows.

136  
137 Although soil storage may not be a major factor in attenuating flows, micro-relief elements (Kellner and  
138 Halldin, 2002) and land cover (Weiss, 1998) both significantly affect runoff as they can provide local  
139 storage and increase the effective roughness of the surface. Additionally, pipes are also often observed in  
140 blanket peats and can couple the shallow acrotelm with the deeper catotelm, contributing between 10-  
141 30% of the total flow (Holden and Burt, 2002b), although their relative contribution to runoff is lower  
142 under saturated conditions, due to the dominance of overland flow processes (Holden, 2005).

143  
144 The saturated hydraulic conductivity ( $K_s$ ) of peat soil is observed to reduce with depth (Clymo, 2004;  
145 Holden et al., 2001; SurrIDGE et al., 2005; Van Seters and Price, 2002), with decreases of as much as five  
146 orders of magnitude by a depth of 0.4 to 0.8m (Bradley, 1996). In the catotelm, high compaction and  
147 greater humification of the material leads to a greater bulk density (Holden and Burt, 2002a) and a  
148 reduction of the voids in the substrate, thereby reducing the saturated hydraulic conductivity. In contrast,  
149 macropores due to voids created from the decaying plant material are particularly important in the  
150 acrotelm and contribute significantly to the higher hydraulic conductivity of this layer (Holden, 2009a).  
151 Shallow throughflow along the boundary of the acrotelm and catotelm is a significant flow mechanism  
152 due to the discontinuity of hydraulic conductivities between the two layers (Holden and Burt, 2003a).

153  
154 Based on literature, a simplified conceptualisation of the hydrological functioning of drained blanket  
155 peatlands has been developed (Figure 1), consisting of three main hydrological components: soil blocks,  
156 drains between soil blocks, and a collector drain. This is used as the basis of a mathematical model to  
157 represent a three-dimensional drained blanket peat hillslope. The parameters in Figure 1, as well as  
158 others that are introduced in the following sections, are defined in the Appendix.

159 **2.2. Mathematical model**

160 Given that the water table in undrained blanket peats is always observed to be close to the surface, and  
 161 the high degree of uncertainty in the parameterisation of a full Richards' equation-based model with  
 162 limited or no unsaturated data, a physics-based unsaturated zone representation has been excluded from  
 163 the model. This has the added benefit of significantly reducing computational time (Pancioni et al, 2003).  
 164 By removing the unsaturated zone, it is assumed that exchanges between the subsurface and the surface  
 165 (i.e. evaporation and infiltration) occur instantaneously; and it is assumed that subsurface lateral fluxes  
 166 can be described using Darcy's law:

$$167 \quad V = -\bar{K}_s(h_s) \frac{\partial h_T}{\partial x} \quad (1)$$

168 where  $V$  is velocity in the downslope direction ( $LT^{-1}$ ),  $\bar{K}_s$  ( $LT^{-1}$ ) is the depth averaged saturated  
 169 hydraulic conductivity,  $h_s$  is the depth of the water table above the impermeable bed (L),  $h_T$  is the total  
 170 hydraulic head (L) and  $x$  is the downslope subsurface ordinate (L). The continuity equation is defined as:

$$171 \quad \bar{\epsilon}(h_s) \frac{\partial h_T}{\partial t} = -\frac{\partial q_s}{\partial x} + i - ET_p \quad (2)$$

172 where  $\bar{\epsilon}$  ( $L^3L^{-3}$ ) is the depth averaged effective porosity,  $q_s$  is the unit width subsurface flux ( $L^2T^{-1}$ ) and  
 173  $i$  and  $ET_p$  ( $LT^{-1}$ ) are exchange terms representing the fluxes across the peat surface due to infiltration and  
 174 evaporation respectively. Decomposing the total hydraulic head ( $h_T$ ) into a fixed component related to the  
 175 slope and a variable component,  $h_s$ , and making the Dupuit-Forcheimer approximation that the flow lines  
 176 are always parallel to the slope, then:

$$177 \quad \frac{\partial h_T}{\partial x} = \frac{\partial h_s}{\partial x} - \tan \theta_s \quad (3)$$

$$178 \quad q_s(x, t, x_d) = -\bar{K}_s(h_s) h_s \left( \frac{\partial h_s}{\partial x} - \tan \theta_s \right) \quad (4)$$

179 where  $\theta_s$  is the site slope. Substituting equation 4 into equation 2 gives the Boussinesq equation:

$$180 \quad \bar{\epsilon}(h_s) \frac{\partial h_s}{\partial t} = \frac{\partial}{\partial x} \left( \bar{K}_s(h_s) h_s \frac{\partial h_s}{\partial x} \right) - \tan \theta_s \frac{\partial (\bar{K}_s(h_s) h_s)}{\partial x} + i - ET_p \quad (5)$$

181 The more commonly used version of the Boussinesq equation (e.g. Beven, 1981; Childs, 1971;  
 182 Henderson and Wooding, 1964; Verhoest et al., 2002) can be derived from equation (5) by assuming  
 183 constant  $K_s$  and using a transformation of  $h_s' = h_s / \cos(\theta_s)$  and  $x' = x / \cos(\theta_s)$  (where  $x'$  and  $h_s'$  are the  
 184 rotated distance and water table height measures). The gravitational frame of reference was chosen here  
 185 to assist in the coupling between the subsurface, overland and drain flows and also allows the drain walls  
 186 to remain vertical. Importantly, the Boussinesq equation still retains dependence on the downslope  
 187 boundary condition, which will be significant once the model is adapted to represent blocked drains. In  
 188 their comparison study of the performance of the Boussinesq equations compared with a full Richards'  
 189 equation representation, Pancioni et al. (2003) concluded that the Boussinesq equation was able to  
 190 successfully capture the shapes of the storage and outflow profiles, particularly for low air-entry pressure  
 191 soils under draining conditions. Given the typically low air entry pressure of the acrotelm (Letts et al,  
 192 2000), the benefits of reduced parameterisation for the Boussinesq equation are likely to outweigh the  
 193 performance benefits of a Richards' equation representation.

194  
 195 The acrotelm-catotelm layering is represented in the model through depth-averaged saturated hydraulic  
 196 conductivity  $\bar{K}_s$  and depth-averaged porosity  $\bar{\epsilon}$  defined by

$$197 \quad \bar{K}_s(h_s) = \frac{\int_{z=0}^{z=h_s} K_s(z) dz}{h_s} \quad (6)$$

198 and

$$199 \quad \bar{\epsilon}(h_s) = \frac{\int_{z=0}^{z=h_s} \epsilon(z) dz}{h_s} \quad (7)$$

200 This depth-averaging provides an approximation of the dual layer system for application in the one-  
 201 dimensional Boussinesq equation. As the model solution is sensitive to discontinuities in the hydraulic  
 202 conductivity a smoothing function is used to describe the variation of hydraulic conductivity with depth:

$$203 \quad K_s(z) = K_{sc} + (K_{sa} - K_{sc}) (1 + \tanh[(z - d_c) / 100]) / 2 \quad (8)$$

204 where  $z$  is the coordinate measured vertically from the impermeable lower boundary,  $K_{sc}$  is the saturated  
 205 hydraulic conductivity of the catotelm,  $K_{sa}$  is the saturated hydraulic conductivity of the acrotelm, and  $d_c$

206 is the thickness of the catotelm. A step function is used to describe the variation of effective porosity  
207 with depth:

$$\begin{aligned} \varepsilon(z(z \leq d_c)) &= \varepsilon_c \\ \varepsilon(z(z > d_c)) &= \varepsilon_a \end{aligned} \quad (9)$$

209 where  $\varepsilon_c$  is the effective porosity of the catotelm and  $\varepsilon_a$  is the effective porosity of the acrotelm.

210 Examples of these relationships are shown in Figure 2.

211  
212 Natural soil pipes have not been explicitly represented in the model, as the data required to parameterise  
213 a pipe model are unlikely to be available for typical model applications; pipe flow contributions are  
214 assumed to be accounted for in the acrotelm hydraulic conductivity. As hydraulic conductivities are  
215 known to be very low at depth (Letts et al., 2000), a zero-flux boundary is imposed at the depth of the  
216 drains. Fluxes into the peat, represented by  $i$  in Equation 5, are firstly from any surface water  
217 (reinfiltration at a maximum rate equal to the saturated hydraulic conductivity), and then directly from  
218 rainfall (snow is not explicitly represented). The rainfall infiltration rate is set at the smaller of the  
219 rainfall rate or the saturated hydraulic conductivity of the upper layer. When the soil is saturated no  
220 infiltration is allowed, due to the no-flux condition at the lower boundary. Infiltration and saturation  
221 excesses are added to the overland flow. For the peat blocks, water is firstly evaporated at the potential  
222 rate from any surface water ( $ET_{OF}$ ), and then from the acrotelm ( $ET_p$ ). Soil evaporation is assumed to  
223 cease when the water table is below the acrotelm. Evaporation from the drains and collector drain ( $ET_d$   
224 and  $ET_c$ ) occurs at the potential rate while water is present.

225  
226 Overland and channel flows are represented by the kinematic wave equation, an approximation of the  
227 Saint Venant equations of gradually varied unsteady flow commonly used for representing surface flow  
228 dynamics (Singh, 1996). The approximation neglects the acceleration and pressure terms in the full  
229 equations, replacing the momentum equation with a steady state depth-discharge relationship. The  
230 general form of the kinematic wave equation is:

$$231 \quad \frac{\partial H}{\partial t} = -\frac{\partial Q}{\partial y} - Sink \quad (10)$$

232 where  $H$  is the flow depth (L),  $Q$  is the unit width flux ( $L^2T^{-1}$ ), *Sink* represents sink and source terms for  
 233 the channel ( $LT^{-1}$ ) and  $y$  is a distance ordinate (L). When applied to the drain, collector drain and  
 234 overland flow, the following three equations are generated:

235 Drain:

$$236 \quad \frac{\partial h_d}{\partial t} = -\frac{\partial q_d}{\partial x_d} + (Rain - ET_d) + \frac{\partial}{\partial x_d} \left( (q_s(end, t, x_d) - q_s(1, t, x_d) + q_{OF}(end, t, x_d)) \frac{\Delta x_d}{W_d} \cos \beta_d \right) \quad (11a)$$

237 Collector drain:

$$238 \quad \frac{\partial h_c}{\partial t} = -\frac{\partial q_c}{\partial x_c} + (Rain - ET_d) + \frac{\partial(q_d(end, t))}{\partial x_c} \quad (11b)$$

239 Overland flow:

$$240 \quad \frac{\partial h_{OF}}{\partial t} = -\frac{\partial q_{OF}}{\partial x} + (Rain - ET_{OF} - i) \quad (11c)$$

241 where  $h_d$  is the drain flow depth (L),  $h_c$  is the collector drain flow depth (L),  $h_{OF}$  is the overland flow  
 242 depth (L), *Rain* is the unit area rainfall ( $LT^{-1}$ ),  $q_{OF}$  is the unit width overland flow ( $L^2T^{-1}$ ),  $q_d$  is the unit  
 243 width drain flow ( $L^2T^{-1}$ ),  $W_d$  is the width of the drain (L),  $x_d$  is the drain ordinate (L) and  $x_c$  is the  
 244 collector drain ordinate (L).

245  
 246 The depth-discharge relationship for the drains was represented by the Manning equation, as friction  
 247 factors quoted in the literature are more commonly Manning's roughness coefficient values. The depth-  
 248 discharge relationship for the drains is:

$$249 \quad q_d(x_d, t) = \frac{h_d \left( \frac{W_d h_d}{(W_d + 2h_d)} \right)^{2/3} \sqrt{\tan(\theta_d)}}{n} \quad (12)$$

250 where  $n$  is the Manning's roughness coefficient and  $\theta_d$  is the slope of the drain, where

251  $\theta_d = \sin^{-1}(\sin \theta_s \sin \beta_d)$ . For the collector drain:

$$252 \quad q_c(x_c, t) = \frac{h_c \left( \frac{W_d h_c}{(W_d + 2h_c)} \right)^{2/3} \sqrt{\tan(\theta_s)}}{n} \quad (13)$$

253

254 In order to utilise data in Holden et al. (2008) for depth varying overland flow friction factors, the  
255 overland flow depth-discharge relationship is calculated using a Darcy-Weisbach equation, given by:

$$256 \quad q_{OF}(x, t, x_d) = h_{OF} \sqrt{\frac{8g \tan(\theta) h_{OF}}{f}} \quad (14)$$

257 where  $g$  is the acceleration due to gravity ( $9.81 \text{ ms}^{-2}$ ) and  $f$  is the Darcy-Weisbach friction factor. Holden  
258 et al. (2008) investigated values of  $f$  for four different land cover types, which in order of increasing  
259 roughness were: bare (Ba), *Eriophorum* (E), *Eriophorum/Sphagnum* mix (E/S) and *Sphagnum* and  
260 *Juncus* (S/J).  $f$  was also found to vary with overland flow depth. The mathematical relationship between  $f$   
261 and depth proposed by Holden et al. (2008) has a discontinuity in the relationship at approximately 1cm  
262 and  $f$  tends to infinity as the overland flow depth tends towards zero. Both of these properties cause  
263 numerical difficulties when introduced into the continuous simulations. Therefore a continuous  
264 polynomial that passes through the origin was identified for each land cover type with the general form  
265  $f(h_{OF}) = ah_{OF} + bh_{OF}^2$ , where parameters  $a$  and  $b$  were optimised to closely recreate the original data.  
266 Parameter  $b$  could be described as a function of  $a$ ; the final relationship used is  $f(h_{OF}) = ah_{OF} -$   
267  $(2.21a + 3.82)h_{OF}^2$ , with values of  $a$ : (Ba) 20.79, (E) 5.05, (E/S) 3.48 and (S/J) 1.90. Parameter  $a$  was used  
268 as a proxy for  $f$  for the purpose of model calibration and sensitivity analysis.

269

270 The resulting model couples four one-dimensional models that represent respectively subsurface,  
271 overland flow, drain flow and collector drain flow (Figure 1). The one-dimensional models are run  
272 simultaneously with feedbacks between the subsurface and surface through the infiltration and  
273 evaporation terms, and between the subsurface and the drains through the drain depth and seepage face  
274 water level. By limiting the model to four one-dimensional models rather than a fully integrated three-  
275 dimensional model, some of the computational demands of the modelling procedure are reduced  
276 (assuming that fewer nodes and fewer equations will lead to reduced computational time) and the  
277 parameterisation of the model can be limited to those parameters for which information can be taken  
278 from the literature (such as the saturated hydraulic conductivity and surface roughness). The model uses

279 inputs of rainfall and potential evaporation, and outputs flow and water depths throughout the model  
280 domain.

281  
282 The model space is discretised into a number of soil blocks (Figure 1), which are bounded upstream and  
283 downstream by drains. The block lengths tested ranged from 5m (close drain spacing) to 500m (to  
284 simulate intact peatland). The model space domain may include a large number of blocks, depending on  
285 the application. Although the drains may be at any angle relative to the contours, the soil blocks are  
286 always aligned downslope, meaning that surface and subsurface flow in the block are always  
287 perpendicular to the contours and parallel to the edge of the block. In this way, flow paths on and in the  
288 soil block may be represented by the single dimension and there is no exchange flow between the soil  
289 blocks. This representation neglects any cross-slope flow paths that may be present.

290  
291 The partial differential equations to describe the variation of flow depths with time for each of the one-  
292 dimensional models were discretised in space using finite differences. The resulting ordinary differential  
293 equations were then integrated in time using Matlab's ODE15s solver (Shampine and Reichelt, 1997;  
294 Shampine et al., 1999). The solver uses an adaptive time grid, which limits the numerical error associated  
295 with each time step to within a user defined tolerance. For the soil block and overland flow calculations,  
296 nodes in the x-direction are in a  $\log_{10}$  space, allowing nodes to be more closely spaced toward the  
297 boundaries. By using a varying x-spacing, computational efficiency can be increased, by focusing nodes  
298 in the regions of rapidly varying flows.

### 299 **3. Model calibration and testing**

#### 300 **3.1. Case study application**

301 Oughtershaw Beck, a tributary of the River Wharfe, is a catchment of approximately 13.8 km<sup>2</sup> (Lane et  
302 al., 2004) located at 54°13'54" N, 2°15'09" W, in the Yorkshire Dales, Northern England (Figure 3). The  
303 average annual rainfall is 1850mm (Wallage et al., 2006). The catchment ranges in elevation from 353m  
304 at the outlet to 640m, and is primarily blanket peat with an average thickness of 2m. The catchment is

305 underlain by carboniferous limestone and millstone grit that is covered with a glacial boulder clay  
306 deposit (Wallage et al., 2006). Open cut drainage was installed over a large portion of the catchment in  
307 the 1960s. There was no maintenance of the drains in the intervening period, but Holden et al. (2007)  
308 surveyed the drains in the area, finding that most had either remained the same dimensions as when cut  
309 or had eroded; there were very few that had naturally infilled or become vegetated.

310

311 A monitoring programme ran from December 2002 until August 2004, consisting of 6 boreholes in a  
312 transect across a drained peatland site within the catchment (Figure 4a), with water table depths below  
313 the surface recorded at approximately 10 minute intervals. The boreholes were monitored continuously  
314 over a 419 day period starting on 17<sup>th</sup> February 2003. A 25° V-notch weir was located in a drain  
315 approximately 32 m downstream of the borehole transect (see Figure 4); the notch was 28cm above the  
316 base of the drain and water level measurements were taken at approximately 5 minute intervals. The weir  
317 equation, calibrated in-situ, is  $Q_w = 0.21 h_w^{2.3}$ , where  $Q_w$  ( $\text{m}^3 \text{s}^{-1}$ ) is weir flow and  $h_w$  (m) is water level  
318 over the crest. 304 days of reliable observations are available during the 21 month period. Because the  
319 field experiment was not originally designed to support a physics-based model, a detailed survey of the  
320 site was not completed prior to the removal of field equipment; therefore information regarding exact  
321 ground surface heights is unknown. A transect survey across the site in the approximate location of the  
322 boreholes indicates that the ground surface level fluctuates by up to 10cm around the average slope of the  
323 site. The schematic map of the site, shown in Figure 4a, is based on information from aerial photographs  
324 and topographic maps. A rain gauge was located approximately 300m from the site, with measurements  
325 made at 15 minute resolution. As evaporation data were not available for the location, an approximate  
326 time series of daily potential evaporation was synthesised using the EARWIG weather generator (Kilsby  
327 et al., 2007). The dataset is unique in its simultaneous high resolution measurements of rainfall, drain  
328 flow and water table in blanket peat and therefore provides an important opportunity to calibrate and test  
329 the model performance.

330

331 The model boundaries were defined by the drains at the top and bottom of the transect, the weir at the  
332 outlet and the upstream end of the central drain (Figure 4b). 10 soil blocks were used in the simulation (5

333 upslope and 5 downslope from the central drain), each with 20 nodes, with spacing of these nodes  
334 ranging from 40cm near the drain to 3.5m in the centre of the soil block. Borehole locations were  
335 explicitly added as nodes, to avoid interpolation errors when comparing the model output against  
336 observations. The original model configuration was altered slightly in order to incorporate the routing  
337 effect of the weir: the drain upstream of the weir was modelled as a reservoir with outflows set by the  
338 weir equation measured in the field. This assumes that the residence time in this drain is dominated by  
339 the storage effect of the weir, and that travel time of the wave is negligible compared to the simulation  
340 output time step, which is considered reasonable because of the short drain length.

341  
342 The model was calibrated by performing a Monte Carlo analysis. 2000 random samples were taken from  
343 the *a priori* parameter ranges shown in Table 1. The calibrated model parameters were: the acrotelm and  
344 catotelm hydraulic conductivities, the thickness of the acrotelm, the angle of the drain, the surface slope  
345 and the type of land cover. Some of the *a priori* ranges were more easily constrained (i.e. the slope and  
346 drain angle) as there was some knowledge about these parameters from information such as maps and  
347 aerial photographs. However, we chose not to fix these parameters, in order to investigate the parameter  
348 sensitivity and also to reflect the uncertainty in this information. The drain length was fixed at 46m based  
349 on the results of a long term mass balance, and the acrotelm and catotelm porosities were set as functions  
350 of their respective hydraulic conductivities following the relationship presented by Letts et al. (2000).  
351 Simulations were then performed for each of the *a priori* parameter sets for a 50 day calibration period  
352 from 24 September 2003 with a preceding 50 day model warm up period (not used for comparison  
353 against the observations) to allow sufficient time for the model behaviour to become independent of the  
354 user-defined initial conditions. The simulations took 6-10s per simulation day using an Intel Core 2 Duo  
355 Processor (E6850, 3.00 GHz).

356  
357 The observed data points were interpolated to the same time samples as the model output (10 minutes).  
358 The model performance was determined for each parameter set using the Root Mean Square Error  
359 (RMSE) for observed discharges (over all the parameter sets RMSE ranges from 0.049 to 0.095 l/s), and  
360 for water table depths for all six boreholes (RMSE ranges from 0.021 to 0.161 m). None of the sampled

361 parameter sets could simultaneously optimise the RMSE for all seven sets of observations. In order to  
362 accommodate the multi-objective nature of the problem and also recognising the uncertainty in the data  
363 and the model, rather than performing verification and predictions with a single “optimal” parameter set,  
364 the parameter sets considered most consistent with the observed hydrology of the site are selected. These  
365 are referred to here as the “*behavioural*” parameter sets (B). The behavioural parameter sets are selected  
366 by firstly taking only the best 5% for the weir flow simulations (100 parameter sets), then further  
367 reducing this set by keeping only the 50 parameter sets that had the best average RMSE for all six  
368 boreholes. Less emphasis is placed on the borehole observations in this combined criteria because our  
369 primary interest is to replicate peak flow hydrographs, and as there is inevitable uncertainty in the  
370 borehole simulations associated with heterogeneity as well as the uncertainty related to the inexact  
371 datums from which the borehole measurements were made. The selection of the criteria was arbitrary;  
372 however it achieved the purpose of constraining the model towards the observed behaviour within an  
373 uncertainty analysis framework.

374

375 Figure 5 shows the confidence limits of the predictions obtained using the *a priori* parameter sets and  
376 those obtained using the *behavioural* parameter sets, plotted with observed weir and borehole data for the  
377 largest event during the calibration period. This shows that the behavioural parameter sets give good  
378 performance during the main flow peak and demonstrates that non-behavioural parameter sets were  
379 typically rejected as they produced soil conditions that were too dry preceding the onset of the rainfall  
380 event and therefore tended to underestimate the first peak. Following the flood peak, all simulations  
381 reflect saturated conditions with the water table at the ground surface; the observations reflect a similar  
382 water table level, fluctuating between -2cm and the surface.

383

384 To test the model outside the calibration period, simulations using only the *behavioural* parameter sets  
385 were performed for the entire observation period (Figure 6). Regions of missing data in Figure 6 are  
386 periods when observations were not made, and periods with missing simulations are periods where  
387 rainfall data were not recorded. Figure 7 illustrates a period of relatively poor performance and high  
388 uncertainty in the transition from a dry to wet period. In this period, the observed rewetting (the time it

389 took for the water table to increase by approximately 10cm) took approximately 3 hours according to the  
390 observations, whereas in the simulation it took approximately 1 day (although the simulations did react  
391 earlier). For the second flow peak, the upper bound reflects the observations; however, the lower bound  
392 indicates no flow. Once the soil became saturated, the third peak shows that the simulation improved  
393 significantly, although the lower bound prediction is only approximately 40% of the observed flow and is  
394 also delayed by approximately 45 minutes.

395  
396 Figure 8 shows good flow performance and reduced uncertainty in a consistently wet period. During this  
397 period the water table was always very close to the surface (<5cm) in both the observations and the  
398 model outputs. Figure 6 demonstrates that ground water levels are generally well predicted in the winter  
399 time, when evaporation is low and the water table is very close to the surface. However, during summer  
400 periods, the magnitude of the drawdown tends to be under-predicted and the time for rewetting tends to  
401 be over-predicted. Predictions for the borehole located 10cm upstream from the drain were consistently  
402 worse than those in the centre of the upslope soil block.

403  
404 The *behavioural* parameter sets can also be used to examine the sensitivity of the model to each of the  
405 parameters, by making comparisons between the frequency distributions of the *behavioural* parameters  
406  $F(\theta_x|B)$  and the frequency distributions of the *a priori* parameter  $F(\theta_x)$  (following the approach of Spear  
407 and Hornberger, 1980). Figure 9 shows the cumulative distribution functions (cdfs) of the *a priori* and  
408 *behavioural* distributions for each parameter; the greater the deviations of the behavioural cdfs from the  
409 *a priori* cdfs, the more sensitive the model prediction is to the parameter. The significance and magnitude  
410 of the difference between these distributions (and therefore the sensitivities) is quantified using the  
411 Kolmogorov-Smirnov (KS) test (see McIntyre et al. 2003). All behavioural parameter distributions were  
412 significantly different from the *a priori* parameter distributions at the 95% confidence interval. For the  
413 parameter ranges tested in this example, the parameters ordered from most sensitive to least sensitive,  
414 based on their KS test statistic values, are: acrotelm saturated hydraulic conductivity ( $K_{sa}$ ), acrotelm  
415 thickness ( $d_a$ ), drain angle ( $\beta_d$ ), catotelm saturated hydraulic conductivity ( $K_{sc}$ ), land cover ( $a$ ) and site  
416 slope ( $\theta_d$ ). The model sensitivity to the evapotranspiration was also tested by running 10 parameter sets,

417 randomly selected from the original 2000 parameter sets, each for five different EARWIG stochastic  
418 realisations for a 150 day period. The mean difference in RMSE between the best performing and worst  
419 performing simulations for each parameter set was 0.0023 l/s for the flow simulations and 0.0036 m for  
420 the water table simulations. This variation was considered to have little significance on the selection of  
421 behavioural parameter sets.

### 422       **3.2.       Generalised parameter space response**

423 The model performance in the case study application suggests that the model captures the key processes  
424 in drained blanket peatlands under wet conditions. For sites that may be modelled with the same structure  
425 but different parameter values, the model was used to explore aspects of hydrological response  
426 throughout the potential parameter space. In these simulations, the original model structure shown in  
427 Figure 1 was used, rather than the version adapted to accommodate the weir. It is assumed that all  
428 possible surface roughnesses for peatland sites can be represented by values of  $a$  between the smoothest  
429 (Ba) and roughest (S/J) land cover types. The parameter ranges for this broader exploration are shown in  
430 Table 1. This allows a qualitative validation of the model results relative to responses reported in the  
431 literature for a range of sites as well as providing a more general picture of the sensitivity of the flow  
432 peaks to the model parameters.

433  
434 The model parameter space was quantised and simulations performed for all the possible parameter  
435 combinations. The model domain was fixed to a 500m x 500m area, and tested with seven design storms  
436 taken from the Flood Estimation Handbook (Robson and Reed, 1999), assuming a winter profile. The  
437 seven events were: 10 year return period with 1 hour duration, 10 year 2 hour, 10 year 6 hour, 10 year 12  
438 hour, 10 year 18 hour, 2 year 12 hour and 50 year 12 hour. As only large design storms were examined,  
439 evaporation was not included in the model. Initial water table levels were set as the steady state solution  
440 for infinite duration rainfall of  $0.1 \text{ md}^{-1}$  and drains were assumed to be empty. The peak flows were  
441 found to be independent of this choice of initial condition. In order to reduce parameterisation, the depth  
442 averaged hydraulic conductivity was assumed to be constant within each simulation, therefore removing  
443 the acrotelm-catotelm representation. The results from the study are shown in Figure 10. For each

444 sampled value of a parameter  $x_i$  ( $i=1$  to 6 representing the six sampled parameters), the mean of the peak  
445 flow values over all rainfall events and sampled values of the other parameters is calculated and plotted  
446 against  $x_i$ . The  $x_i$  values have been scaled to range between 0 and 1; the hydraulic conductivity is shown  
447 on a log scale.

448  
449 The model behaviour was found to be consistent with observations from the literature. For example, at  
450 high hydraulic conductivities, drainage is found to be very effective in reducing peak flows; with low  
451 hydraulic conductivities (such as in peatlands), drainage is found to increase model peak flows and  
452 decrease times to peak, with the effects generally larger in systems with closer drains and lower  
453 hydraulic conductivities (e.g. Holden et al., 2006; Robinson, 1986; Stewart and Lance, 1991). At very  
454 close drain spacing, the peak model flows begin to reduce, suggesting that spacing contributes to both  
455 increased storage and increased conveyance. Examination of the water table profiles also shows that the  
456 spatial variation in water table depth observed in the field (Coulson et al., 1990; Holden et al., 2006) is  
457 also replicated in the model.

#### 458 **4. Discussion**

459 A new hydrological model has been presented for drained blanket peats that can explicitly represent  
460 varied drainage networks and the water table response between these drains. The simplified physics-  
461 based model allows for the exploration of the internal model behaviour, whilst still being relatively  
462 computationally efficient. High quality data from small scale peatland sites are quite limited, and as  
463 model complexity increases, there is less likelihood that suitable observational data are available to  
464 constrain the model parameters (Freer et al., 2004). Despite the limited complexity of the new model, and  
465 the fact that the dataset used for calibration is unique in the UK for the high level of information that it  
466 contains about peatlands, there are still challenges in the calibration, in particular, simultaneously  
467 optimising the model performance against individual observation time series. There are many possible  
468 causes for inconsistency between model outputs and observations, related to the model conceptualisation  
469 as well as the quality or suitability of the observations.

470

471 Our approach to model calibration in this paper has taken into account responses that it would be  
472 reasonable to expect the model to simulate given its relative simplicity. A spatially homogeneous  
473 representation of site properties is unlikely to provide consistently accurate representations of multiple  
474 point estimates of water table levels. We also note that without a detailed survey of the site, and only the  
475 site averaged slope to work from, water table measurements made from a ground surface reference level  
476 may have several centimetres of error in them. In the field, it is also difficult to precisely define the  
477 surface of a peat, as in reality, the change from peatland vegetation to acrotelm is more of a continuum  
478 than a discrete layering. Therefore, the influence of the water table levels was down-weighted in the  
479 calibration so that that the simulated response was considered acceptable if it was broadly consistent with  
480 the general response of the six boreholes. Despite the reduced weighting of the boreholes in the  
481 calibration, they provided important information in the calibration process, particularly in refining the  
482 behavioural range of the slope; without the information from the boreholes, the slope would not have  
483 been identified as a sensitive parameter.

484

485 Even with these challenges, the longer term behaviour of the water table is generally reliably predicted  
486 (see Figure 6), with seasonal variability represented well. However, Figure 6 also highlights the  
487 relatively poor prediction of the water table near the drain edge. This is unsurprising as the assumptions  
488 made in the Boussinesq equation are no longer valid in regions near the drainage ditches, where  
489 streamlines begin to converge and the Dupuit-Forcheimer approximation fails (Bear, 1988). Drain edges  
490 are also modelled as vertical, whereas in reality they will have some degree of incline. Whether distances  
491 to the boreholes are measured from the drain edge at the top or the bottom of the drain will therefore  
492 have an impact on the location of the borehole in the model domain. Near the edges of the peat blocks,  
493 where the water table level is rapidly varying, water table predictions are very sensitive to movement of a  
494 matter of centimetres upslope or downslope of a given location. Should more accurate simulations of the  
495 water table within 1m or less of the drain edge be required, it would be necessary to reassess the  
496 suitability of the Boussinesq equation.

497

498 Despite the inevitable conflict resulting from the desire to accurately represent local scale hydrological  
499 processes and the requirement that the model should be computationally efficient, the model performs  
500 consistently well during wet periods (e.g. Figure 8). Performance during drying periods and the  
501 following recoveries was more poorly represented and had the greatest uncertainty. We assume that the  
502 slower recovery of the water table is probably related to the exclusion of an unsaturated zone  
503 representation, as in reality water stored in the unsaturated zone would add to the infiltrating water to  
504 increase the rate of water table rise. However, we suggest that, in the context of flood response, the loss  
505 of precision for these periods is outweighed by the significant gains in computational time (assuming that  
506 number of model nodes can be taken as a proxy for computational time, (e.g. Pancioni et al, 2003)), and  
507 also note that a poorly constrained complex subsurface representation would be unlikely to provide  
508 greater precision in these periods. It is also important to note that our calibration period was during  
509 winter; therefore it is possible that if there had been suitable data to use for a calibration period in the  
510 summer time, that drying and rewetting of the peat may have been better captured in the behavioural  
511 parameter set.

512  
513 Based on an examination of the response of the modelled flow across the parameter space under large  
514 rainfall events, the model parameter to which the peak flow response is most sensitive is the drain  
515 spacing followed by the hydraulic conductivity. However, at low hydraulic conductivities (e.g. typical of  
516 UK blanket peats) the peak flow is almost independent of the hydraulic conductivity. In that case, apart  
517 from drain spacing, the peak flows are most sensitive to the parameters related to the land surface and  
518 drain roughnesses. This is unsurprising given that the simulations were for large rainfall events, where  
519 any storage in the subsurface could be rapidly filled. The high sensitivity of flow to the roughness  
520 parameters also reflects their high uncertainty. Further field investigations of these parameters (e.g.  
521 Holden et al., 2008) would greatly enhance any hydrological modelling efforts for blanket peatlands.

## 522 **5. Conclusions**

523 The processes and responses associated with drained peatlands have been captured in a new simplified  
524 physics-based model. The model has advantages over previous physics-based and lumped conceptual

525 models, as it provides flexibility in the drainage configurations that can be represented and can provide  
526 outputs of the spatial variability of model internal states. The results of the generalised parameter space  
527 response indicate that peak flows are sensitive to the geometric properties of the hillslope and drainage  
528 configurations, therefore models that are spatially lumped or restricted in their model configuration  
529 cannot as accurately distinguish those sites that pose the greatest flood hazard. The model therefore has  
530 potential in terms of specifically identifying and prioritising areas for flood hazard mitigation measures  
531 in terms of potential reduction of downstream flood risk. The model has been tested against a dataset  
532 from the UK and has been shown to perform well in terms of capturing peak flow responses under  
533 saturated or near-saturated soil moisture conditions. Poorer performance under drier conditions was  
534 explained by lack of an accurate unsaturated zone model, which while not of great concern for flood flow  
535 applications, could restrict the model's usefulness for the exploration of other peat management impacts  
536 on, for example, low flows and water quality. Although the unknown surface levels at the boreholes  
537 created challenges with the simultaneous optimisation of all six boreholes, long term behaviour of water  
538 table levels was reasonably well predicted, and the general water table behaviour was consistent with  
539 observations from other studies. How far the model can be generalised will need to be explored further  
540 through testing against more data sets. The effect of spatial heterogeneity of the model parameters should  
541 also be investigated. The modelling process has helped identify the overland and channel flow roughness  
542 parameters as being particularly important controls on peak flow response. Further field research towards  
543 constraining these parameters is expected to enhance the model performance.

## 544 **6. Acknowledgements**

545 This research was funded by the UK Flood Risk Management Research Consortium Phase 2, EPSRC  
546 Grant EP/F020511/1. Time to work on field data used in this paper was gratefully provided by a Philip  
547 Leverhulme Prize awarded to Joseph Holden. Thank you also to two anonymous reviewers, whose  
548 constructive comments helped us to significantly improve the manuscript.

## 549 **Appendix**

550 List of parameters:

551	$a$	Proxy overland flow friction factor
552	$\beta_d$	Drain angle (Degrees)
553	$\varepsilon_a$	Effective porosity of acrotelm (-)
554	$\varepsilon_c$	Effective porosity of catotelm (-)
555	$\theta_d$	Drain slope (Degrees)
556	$\theta_s$	Site slope (Degrees)
557	$\theta_x$	<i>A priori</i> parameter sets
558	$B$	<i>Behavioural</i> parameter sets
559	$d_a$	Thickness of the catotelm (L)
560	$d_c$	Thickness of the catotelm (L)
561	$ET_c$	Actual evaporation from collector drain ( $LT^{-1}$ )
562	$ET_d$	Actual evaporation from drains ( $LT^{-1}$ )
563	$ET_{OF}$	Actual evaporation from overland flow ( $LT^{-1}$ )
564	$ET_p$	Actual evaporation from peat soil ( $LT^{-1}$ )
565	$f$	Darcy Weisbach friction factor (-)
566	$g$	Acceleration due to gravity ( $9.81 \text{ ms}^{-2}$ )
567	$H$	Generic water depth (L)
568	$h_d$	Depth of water in drain (L)
569	$h_{OF}$	Depth of overland flow (L)
570	$h_T$	Total hydraulic head (L)
571	$h_s$	Depth of water table above impermeable bed (L)
572	$h_w$	Height of water above weir crest (L)
573	$i$	Infiltration ( $LT^{-1}$ )
574	$K_{Sa}$	Saturated hydraulic conductivity of acrotelm ( $LT^{-1}$ )
575	$K_{Sc}$	Saturated hydraulic conductivity of catotelm ( $LT^{-1}$ )
576	$L_C$	Length of the collector drain and site length (L)
577	$L_d$	Length of the drain (L)
578	$n$	Manning's n

579	$Q$	Generic unit width flux ( $L^2T^{-1}$ )
580	$q_c$	Collector drain flow ( $L^2T^{-1}$ )
581	$q_d$	Drain flow ( $L^2T^{-1}$ )
582	$q_{OF}$	Unit flux of overland flow ( $L^2T^{-1}$ )
583	$q_s$	Unit flux of subsurface flow ( $L^2T^{-1}$ )
584	$Q_w$	Weir flow ( $L^3T^{-1}$ )
585	$t$	Time (T)
586	$V$	Generic velocity in downslope direction ( $LT^{-1}$ )
587	$W$	Drain spacing (L)
588	$W_d$	Drain width (L)
589	$x$	Peat block ordinate (L)
590	$x_c$	Collector drain ordinate (L)
591	$x_d$	Drain ordinate (L)
592	$y$	Generic downslope distance ordinate (L)

## 593 **References**

- 594 Ahti, E., 1980. Ditch spacing experiments in estimating the effects of peatland drainage on summer  
595 runoff, Proceedings of the International Symposium on Influence of Man on Hydrological  
596 Regime. IAHS-AISH Publication 130, Helsinki, pp. 49–53.
- 597 Allaby, M. (Editor), 2008. Oxford Dictionary of Earth Sciences. Oxford University Press, Oxford.
- 598 Armstrong, A. Kay, B., McDonald, A. T., Gledhill, S., Foulger, M. and Walker, A., 2010. Peatland drain  
599 blocking reduces dissolved organic carbon loss and discoloration of water; results from a  
600 national survey. J. Hydrol., in press.
- 601 Bear, J., 1988. Dynamics of Fluids in Porous Media. Dover Publications, Mineola, N.Y.
- 602 Beven, K., 1981. Kinematic subsurface stormflow. Wat. Resour. Res., 17(5): 1419-1424.

- 603 Bonn, A., Allott, T.E.H., Hubacek, K. and Stewart, J., 2009. Introduction: drivers of change in upland  
604 environments: concepts, threats and opportunities. In: A. Bonn, T.E.H. Allott, K. Hubacek and J.  
605 Stewart (Editors), Drivers of change in upland environments. Routledge, Oxon, pp. 1-10.
- 606 Bradley, C., 1996. Transient modelling of water-table variation in a floodplain wetland, Narborough  
607 Bog, Leicestershire. *J. Hydrol.*, 185(1-4): 87-114.
- 608 Bragg, O.M., 2002. Hydrology of peat-forming wetlands in Scotland. *Sci. Total Environ.*, 294(1): 111-  
609 129.
- 610 Burke, W., 1967. Principles of drainage with special reference to peat. *Ir. For.* 24: 1-7.
- 611 Childs, E.C., 1971. Drainage of Groundwater Resting on a Sloping Bed. *Wat. Resour. Res.*, 7: 1256-  
612 1263.
- 613 Clymo, R.S., 2004. Hydraulic conductivity of peat at Ellergower Moss, Scotland. *Hydrol. Process.*,  
614 18(2): 261-274.
- 615 Condliffe, I., 2009. Policy change in the uplands. In: A. Bonn, T.E.H. Allott, K. Hubacek and J. Stewart  
616 (Editors), Drivers of change in upland environments. Routledge, Oxon, pp. 59-89.
- 617 Conway, V.M. and Millar, A., 1960. The hydrology of some small peat-covered catchments in the  
618 northern Pennines. *J. Inst. Water Engin.*, 14: 415-424.
- 619 Coulson, J.C., Butterfield, J.E.L. and Henderson, E., 1990. The Effect of Open Drainage Ditches on the  
620 Plant and Invertebrate Communities of Moorland and on the Decomposition of Peat. *J. Appl.*  
621 *Ecol.*, 27(2): 549-561.
- 622 Dunn, S.M. and Mackay, R., 1996. Modelling the hydrological impacts of open ditch drainage. *J.*  
623 *Hydrol.*, 179(1-4): 37-66.

- 624 Evans, M.G., Burt, T.P., Holden, J. and Adamson, J.K., 1999. Runoff generation and water table  
625 fluctuations in blanket peat: evidence from UK data spanning the dry summer of 1995. *J.*  
626 *Hydrol.*, 221(3): 141-160.
- 627 Freer, J.E., McMillan, H., McDonnell, J.J. and Beven, K.J., 2004. Constraining dynamic TOPMODEL  
628 responses for imprecise water table information using fuzzy rule based performance measures. *J.*  
629 *Hydrol.*, 291(3-4): 254-277.
- 630 Henderson, F.M. and Wooding, R.A., 1964. Overland Flow and Groundwater Flow from a Steady  
631 Rainfall of Finite Duration. *J. Geophys. Res.*, 69: 1531-1540.
- 632 Holden, J., 2005. Controls of soil pipe frequency in upland blanket peat. *J. Geophys. Res.*, 110: F01002.
- 633 Holden, J., 2009a. Flow through macropores of different size classes in blanket peat. *J. Hydrol.*, 364(3-  
634 4): 342-348.
- 635 Holden, J., 2009b. Upland Hydrology. In: A. Bonn, T.E.H. Allott, K. Hubacek and J. Stewart (Editors),  
636 Drivers of change in upland environments. Routledge, Oxon, pp. 113-134.
- 637 Holden, J. and Burt, T.P., 2002a. Laboratory experiments on drought and runoff in blanket peat. *Eur. J.*  
638 *Soil Sci.*, 53(4): 675-689.
- 639 Holden, J. and Burt, T.P., 2002b. Piping and pipeflow in a deep peat catchment. *Catena*, 48(3): 163-199.
- 640 Holden, J. and Burt, T.P., 2003a. Hydraulic conductivity in upland blanket peat: measurement and  
641 variability. *Hydrol. Process.*, 17(6): 1227-37.
- 642 Holden, J. and Burt, T.P., 2003b. Hydrological studies on blanket peat: the significance of the acrotelm-  
643 catotelm model. *J. Ecol.*, 91(1): 86-102.
- 644 Holden, J. and Burt, T.P., 2003c. Runoff production in blanket peat covered catchments. *Wat. Resour.*  
645 *Res.*, 39(7): 1191.

- 646 Holden, J., Burt, T.P. and Cox, N.J., 2001. Macroporosity and infiltration in blanket peat: the  
647 implications of tension disc infiltrometer measurements. *Hydrol. Process.*, 15(2): 289-303.
- 648 Holden, J. Chapman, P.J. and Labadz, J.C., 2004. Artificial drainage of peatlands: hydrological and  
649 hydrochemical process and wetland restoration. *Prog. Phys. Geog.*, 28(1): 95-123.
- 650 Holden, J., Evans, M.G., Burt, T.P. and Horton, M.M., 2006. Impact of land drainage on peatland  
651 hydrology. *J. Environ. Qual.*, 35(5): 1764-78.
- 652 Holden, J., Gascoign, M. and Bosanko, N.R. 2007. Erosion and natural revegetation associated with  
653 surface land drains in upland peatlands. *Earth Surface Processes and Landforms*, 32: 1547-1557.
- 654 Holden, J., Kirkby, J., Lane, S. N., Milledge, D. G., Brookes, C. J., Holden, V. and McDonald, A. T.,  
655 2008. Overland flow velocity and roughness properties in peatlands. *Wat. Resour. Res.*, 44:  
656 W06415.
- 657 Ingram, H.A.P., 1978. Soil Layers in Mires - Function and Terminology. *Journal of Soil Science*, 29:  
658 224-227.
- 659 Ingram, H.A.P., 1983. Hydrology. In: Gore, A.J.P. (Ed.). *Ecosystems of the World 4A, Mires: Swamp,*  
660 *Bog, Fen and Moor*, Elsevier, Oxford, pp. 67–158.
- 661 Kellner, E. and Halldin, S., 2002. Water budget and surface-layer water storage in a Sphagnum bog in  
662 central Sweden. *Hydrol. Process.*, 16(1): 87-103.
- 663 Kilsby, C.G., Jones, P. D., Burton, A., Ford, A. C., Fowler, H. J., Harpham, C., James, P., Smith and A.,  
664 Wilby, R. L., 2007. A daily weather generator for use in climate change studies. *Environ.*  
665 *Modell. Softw.*, 22(12): 1705-1719.
- 666 Lane, S. N., 2002. More floods, less rain: changing hydrology in a Yorkshire context. *Regional Review*,  
667 11: 18-19.

668 Lane, S.N., Brookes, C. J., Hardy, R. J., Holden, J., James, T. D., Kirkby, M. J., McDonald, A. T., Tayefi,  
669 V. and Yu, D., 2003. Land management, flooding and environmental risk: new approaches to a  
670 very old question. In Proceedings of the Annual CIWEM Conference, Harrogate, September  
671 2003, 10–12.

672 Lane, S. N., Brookes, C.J., Kirkby, A.J. and Holden, J., 2004. A network-index based version of  
673 TOPMODEL for use with high-resolution digital topographic data. *Hydrol. Process.*, 18(1): 191-  
674 201.

675 Letts, M.G., Roulet, N.T., Comer, N.T., Skarupa, M.R. and Verseghy, D.L., 2000. Parametrization of  
676 Peatland Hydraulic Properties for the Canadian Land Surface Scheme. *Atmos. Ocean*, 38(1):  
677 141-160.

678 McIntyre, N, Wagener, T, Wheater, H, Chapra, S. 2003. Risk-based modelling of surface water quality -  
679 A case study of the Charles River, Massachusetts. *J. Hydrol.*, 274, 225-247.

680 Milne, R. and Brown, T.A., 1997. Carbon in the Vegetation and Soils of Great Britain. *J. Environ.*  
681 *Manage.*, 49(4): 413-433.

682 Newson, M.D. and Robinson, M., 1983. Effects of Agricultural Drainage on Upland Streamflow: Case  
683 Studies in Mid-Wales. *J. Environ. Manage.*, 17(4): 333-348.

684 Paniconi, C., Troch, P.A., van Loon, E.E. and Hilberts, A.G.J., 2003. Hillslope-storage Boussinesq  
685 model for subsurface flow and variable source areas along complex hillslopes: 2.  
686 Intercomparison with a three-dimensional Richards equation model. *Wat. Resour. Res.*, 39(11):  
687 1317.

688 Robinson, M., 1986. Changes in catchment runoff following drainage and afforestation. *J. Hydrol.*, 86(1-  
689 2): 71-84.

690 Robson, A. and Reed, D., 1999. Flood estimation handbook: statistical procedures for flood frequency  
691 estimation. Institute of Hydrology.

- 692 Rubec, C., 2005. The decade of the bog 1994-2004: Global progress on peatland wise use and  
693 conservation. *Suo*, 56(1): 19-26.
- 694 Shampine, L.F. and Reichelt, M.W., 1997. The MATLAB ODE Suite. *SIAM J. Sci. Comput.*, 18(1): 1-  
695 22.
- 696 Shampine, L.F., Reichelt, M.W. and Kierzenka, J., A., 1999. Solving Index-1 DAEs in MATLAB and  
697 Simulink. *SIAM Rev.*, 41(3): 538-552.
- 698 Singh, V.P., 1996. Kinematic wave modeling in water resources. *Surface-water hydrology* John Wiley  
699 and Sons, Inc., Chichester, UK, 1399 pp.
- 700 Spear, R.C. and Hornberger, G.M., 1980. Eutrophication in peel inlet--II. Identification of critical  
701 uncertainties via generalized sensitivity analysis. *Water Res.*, 14(1): 43-49.
- 702 Stewart, A.J. and Lance, A.N., 1983. Moor-draining: A review of impacts on land use. *J. Environ.*  
703 *Manage.*, 17(1): 81-99.
- 704 Stewart, A.J. and Lance, A.N., 1991. Effects of moor-draining on the hydrology and vegetation of  
705 northern Pennine blanket bog. *J. Appl. Ecol.*, 28(3): 1105-1117.
- 706 Surridge, B.W.J., Baird, A.J. and Heathwaite, A.L., 2005. Evaluating the quality of hydraulic  
707 conductivity estimates from piezometer slug tests in peat. *Hydrol. Process.*, 19(6): 1227-44.
- 708 Van Seters, T.E. and Price, J.S., 2002. Towards a conceptual model of hydrological change on an  
709 abandoned cutover bog, Quebec. *Hydrol. Process.*, 16(10): 1965-1981.
- 710 Verhoest, N.E.C., Pauwels, V.R.N., Troch, P.A. and De Troch, F.P., 2002. Analytical Solution for  
711 Transient Water Table Heights and Outflows from Inclined Ditch-Drained Terrains. *J. Irrig.*  
712 *Drain. E-ASCE*, 128: 358.

- 713 Wallage, Z.E., Holden, J. and McDonald, A.T., 2006. Drain blocking: An effective treatment for  
714 reducing dissolved organic carbon loss and water discolouration in a drained peatland. *Sci. Total*  
715 *Environ.*, 367(2-3): 811-821.
- 716 Weiss, R., 1998. Modeling moisture retention in peat soils. *Soil Sci.*, 62(2): 305-313.
- 717 Wheater, H.S., Reynolds, B., McIntyre, N., Marshall, M., Jackson, B., Frogbrook, Z., Solloway, I.,  
718 Francis, O. J. and Chell, J., 2008. Impacts of upland land management on flood risk: multi-scale  
719 modelling methodology and results from the Pontbren experiment, FRMRC Research Report UR  
720 16, Imperial College & CEH Bangor.
- 721

Table 1: Parameter ranges for Oughtershaw Beck Monte Carlo simulations and general sensitivity analysis

Parameter	Ranges for Oughtershaw Beck Monte Carlo Simulations		Ranges for Sensitivity Analysis	
	Lower value	Upper value	Lower value	Upper value
Acrotelm hydraulic conductivity (m/d)	0.1	4	(Depth Averaged) 0.001	(Depth averaged) 10
Catotelm hydraulic conductivity (m/d)	0.001	0.05		
Acrotelm thickness (m)	0.05	0.2	FIXED	
Drain angle (degrees)	10	20	15	60
Surface slope (degrees)	5	10	2	14
Land cover	Sphagnum & Juncus (roughest)	Eriophorum (smoothest)	Sphagnum & Juncus (roughest)	Bare (smoothest)
Manning's n	n/a	n/a	0.2	1.4
Drain spacing (m)	FIXED		5	500

Figures:

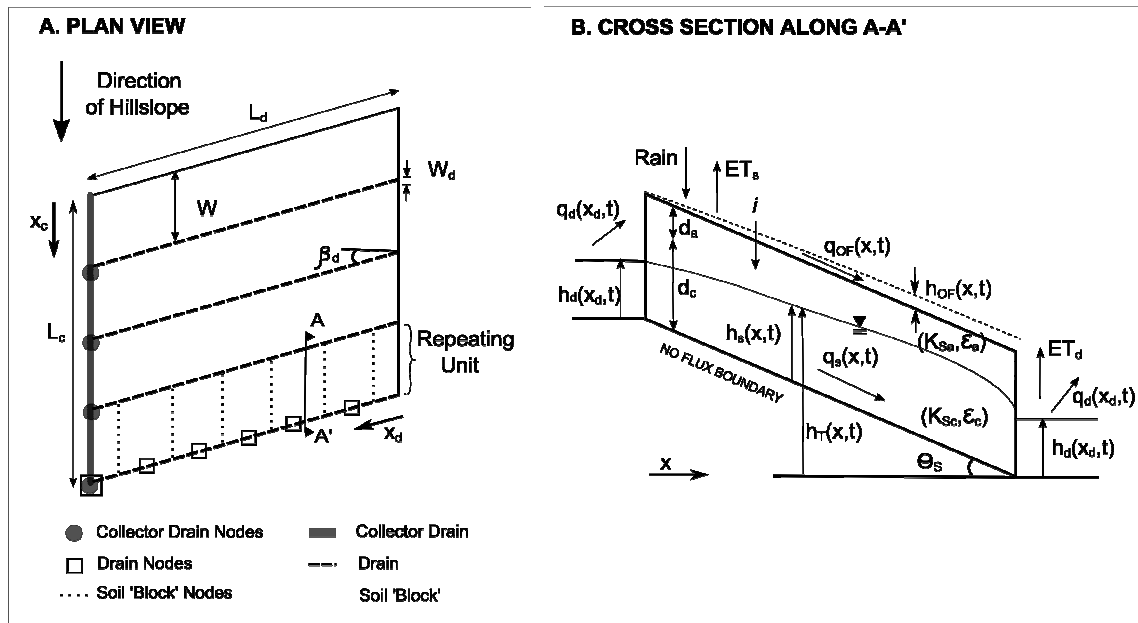


Figure 1: conceptual model of drained peatland

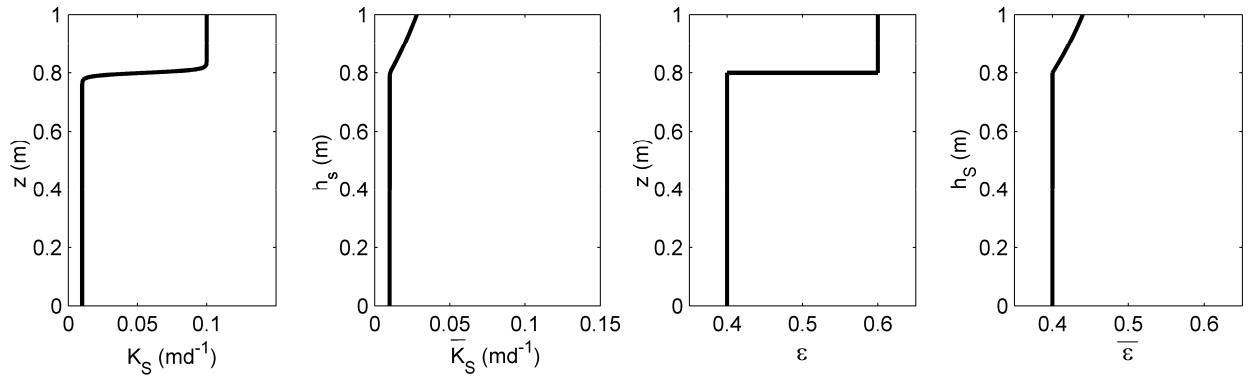


Figure 2. Variation of  $\bar{K}_S$  and  $\bar{\epsilon}$  with  $h_S$ , and variation of  $K_S$  and  $\epsilon$  with  $z$ , given  $K_{Sa}=1 \text{ md}^{-1}$ ,  $K_{Sc}=0.01 \text{ md}^{-1}$ ,  $\epsilon_a = 0.6$ ,  $\epsilon_c = 0.4$ ,  $d_a=0.2\text{m}$  and  $d_c = 0.8\text{m}$

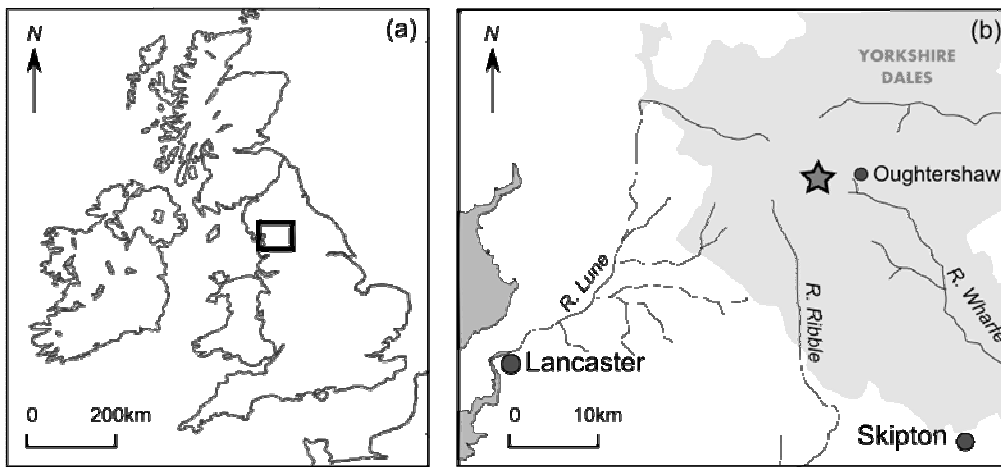


Figure 3: Location map of Oughtershaw Beck; (a) Location within the British Isles (b) Site location within the Yorkshire dales, marked by the star. Major towns in the area are marked with large circles; Oughtershaw is a small hamlet and marked with a small circle.

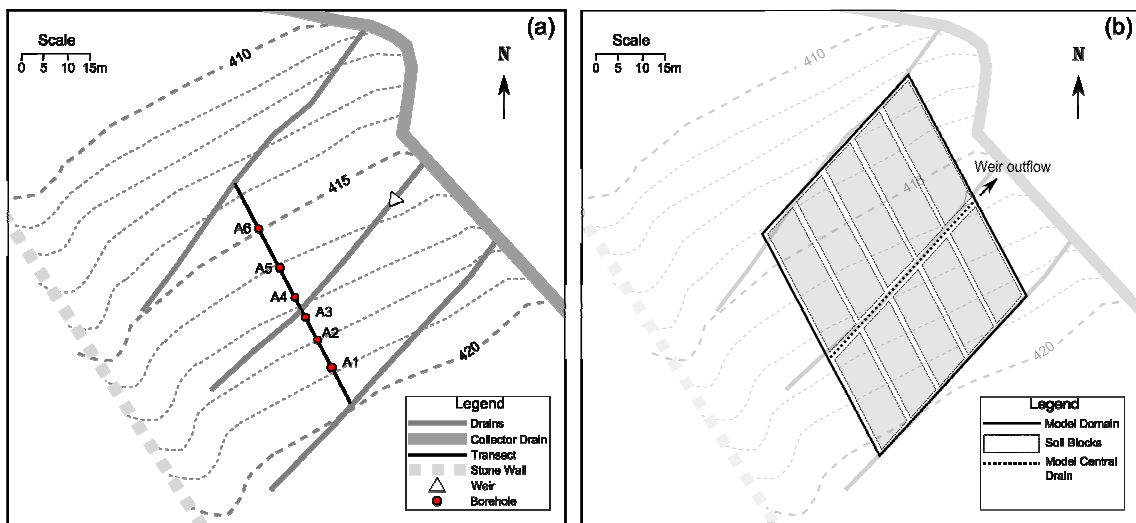


Figure 4: (a) Field site schematic diagram, (b) Model domain and soil blocks

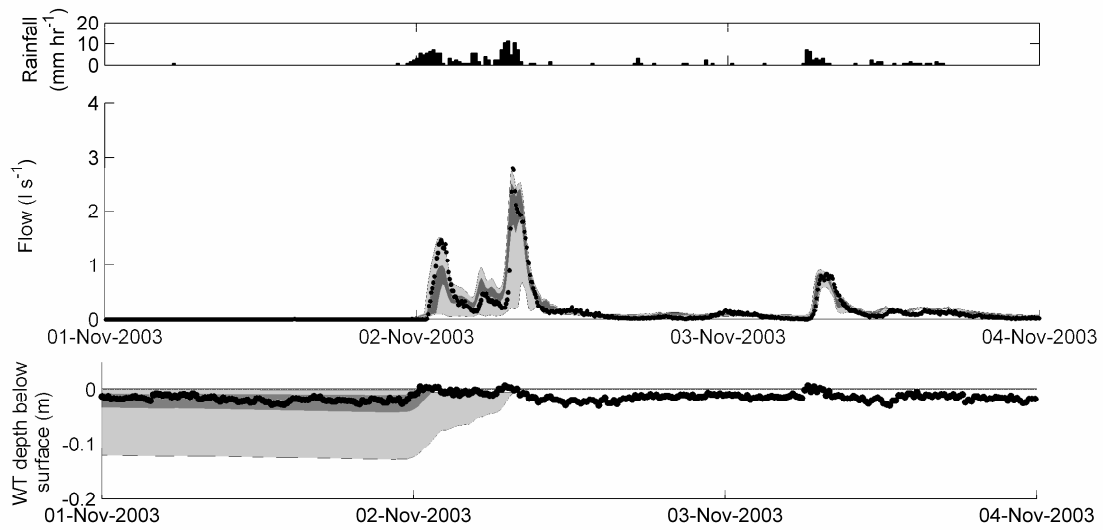


Figure 5: Four day sample from the calibration period, showing the largest peak and water table (WT) depth at borehole A2. Light grey: 90% confidence interval for all simulations; dark grey: 90% confidence interval for behavioural simulations; black dots: observations

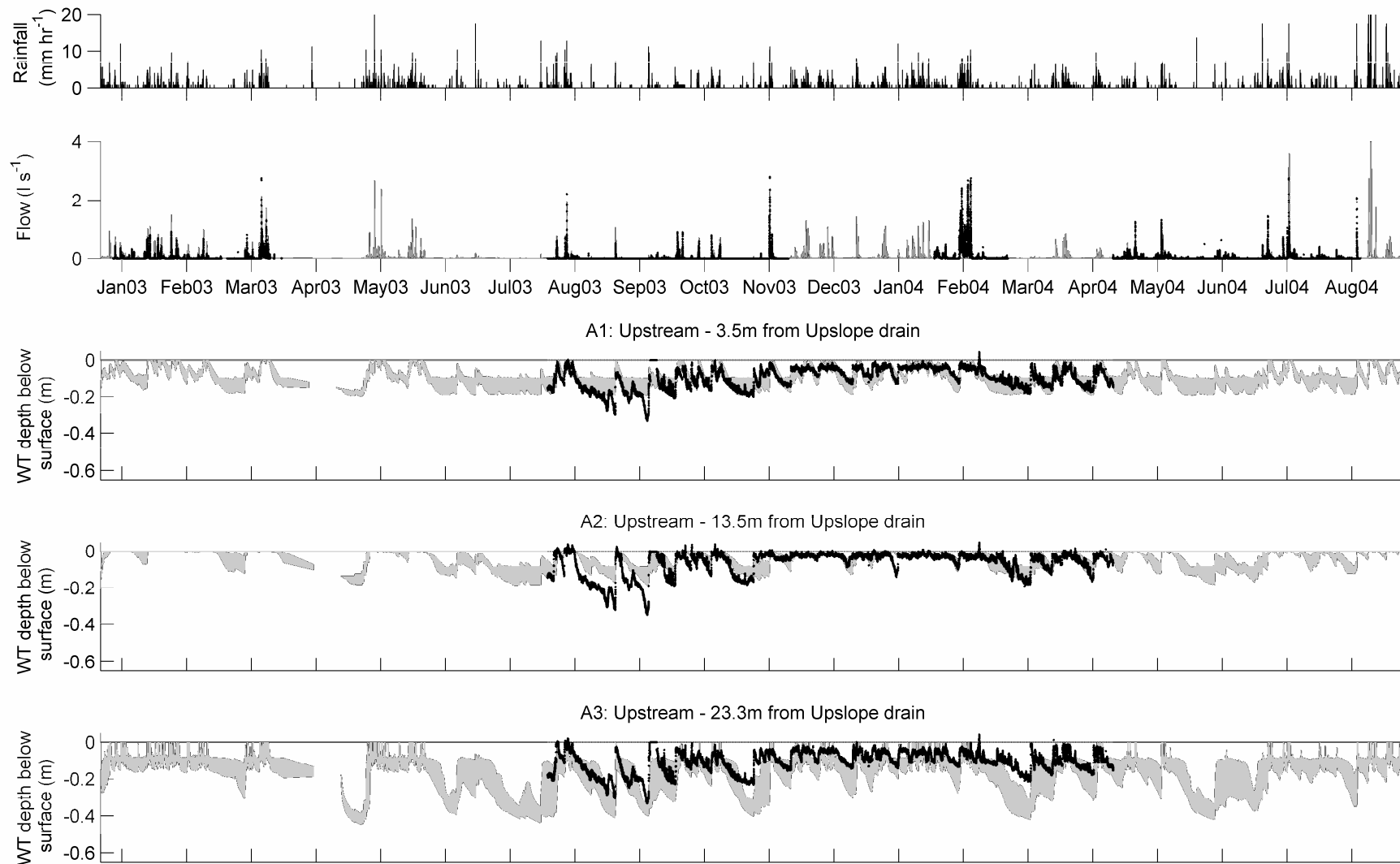


Figure 6: Rainfall, flow and upstream water table depth for the verification period. Grey area: 90% confidence interval of *behavioural* simulations; black line or black dots: observations.

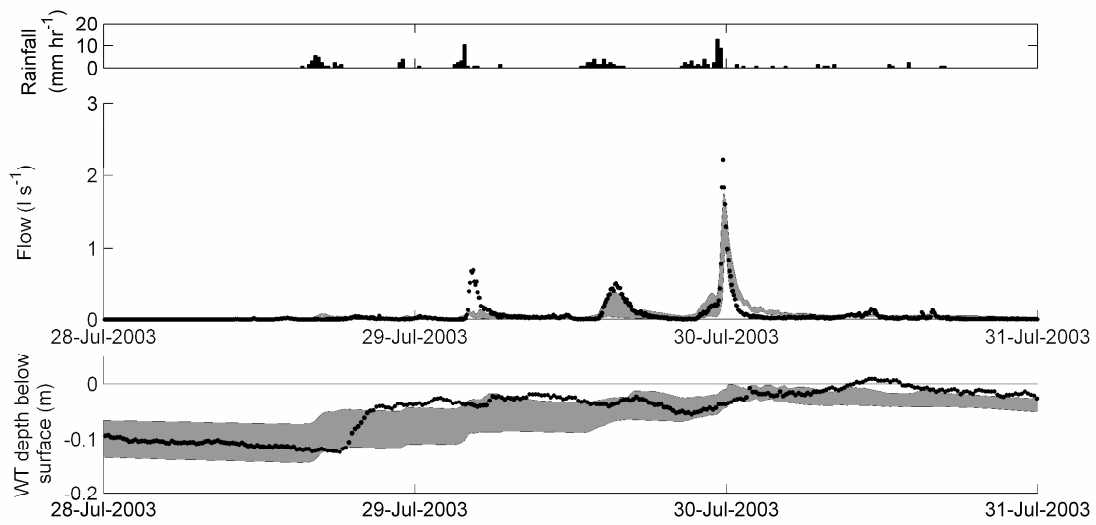


Figure 7: Flow hydrograph and water table (WT) depth for borehole A2 from verification period. Grey area: 90% confidence interval of *behavioural* simulations; black dots: observations.

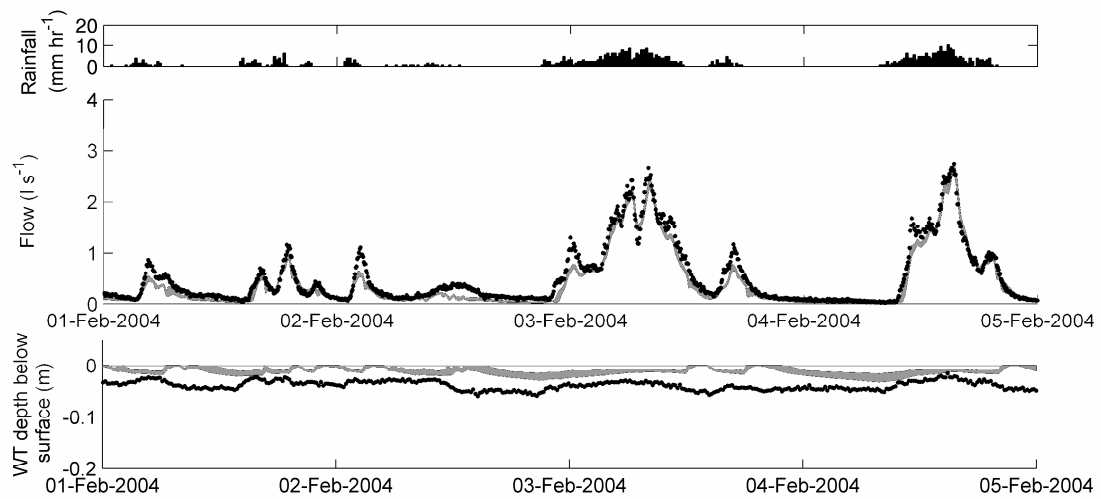


Figure 8: Flow hydrograph and water table (WT) depth for borehole A2 from verification period. Grey area: 90% confidence interval of *behavioural* simulations; black dots: observations

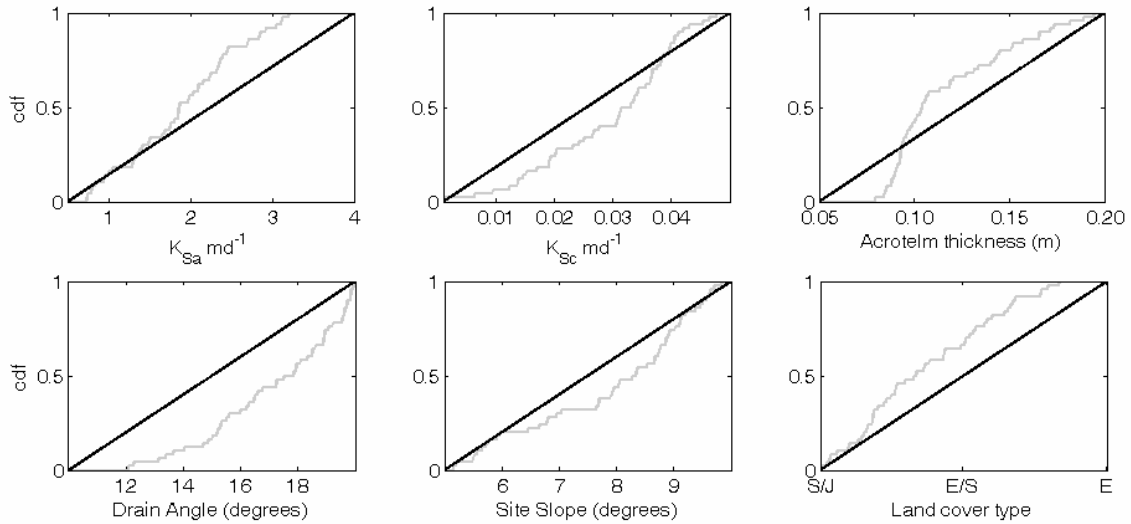


Figure 9: Cumulative density plots of the *a priori* and behavioural parameter distributions. Black line: *a priori* parameter distribution; grey line: behavioural parameter distribution

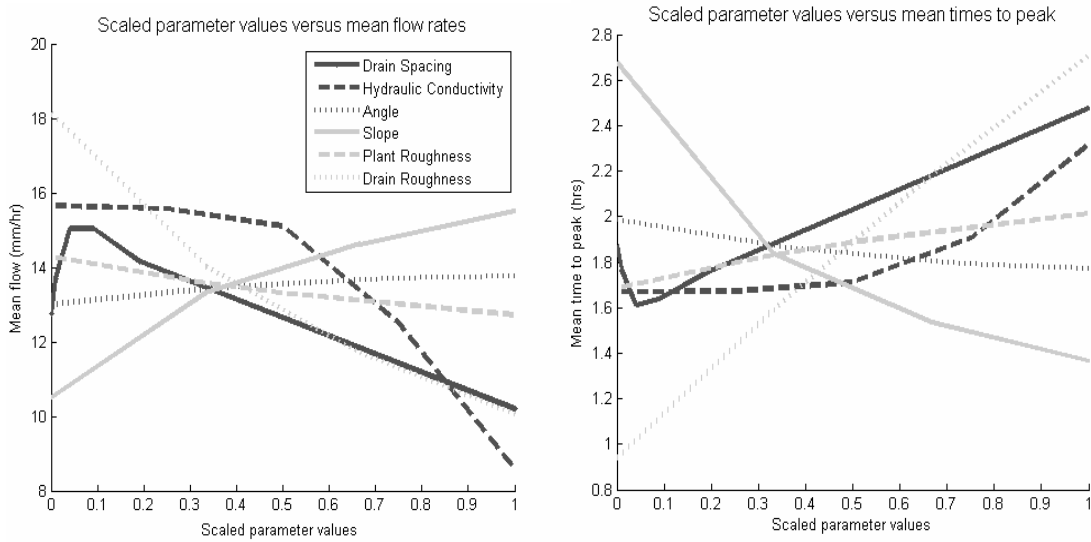


Figure 10: Mean flow rates and mean times to peak versus scaled parameter values